Received: 28 January 2019 | Revised: 9 May 2019 | Accepted: 16 May 2019

DOI: 10.1002/stc.2403

RESEARCH ARTICLE

WILEY

Synergistic and combinatorial optimization of finite element models for monitored buildings

Gaetano Miraglia[1] | Erica Lenticchia[1] | Rosario Ceravolo[1] | Raimondo Betti[2]

[1]Department of Structural, Building and Geotechnical Engineering, DISEG, Politecnico di Torino, Torino, Italy

[2]Department Engineering and Engineering Mechanics, CEEM, Columbia University, New York, NY

Correspondence
Rosario Ceravolo, Department of Structural, Building and Geotechnical Engineering, DISEG, Politecnico di Torino, Italy, c. Duca degli Abruzzi 24, Torino 10129, Italy.
Email: rosario.ceravolo@polito.it

Funding information
DPC-ReLUIS; Compagnia di San Paolo

Summary

This paper investigates the use of rank aggregation strategies for the finite element model calibration of monitored masonry structures subjected to earthquakes. Ranking is used to obtain optimal results from several competing optimization strategies, with the final aim of establishing a numerical model of reference to support the existing monitoring systems installed on the structures. For the tuning of the model, different optimization methods are currently employed (i.e., genetic optimization, particle swarm optimization, and simulated annealing optimization), which can provide an initial nonunique definition of the structural parameters. Starting from the results obtained from selected updating methods, a combinatorial parameter selection is proposed to define the best finite element model among several optimal results. In this case, the ranking problem is solved by using a Plackett-Luce model-based strategy. The calibrated model is a useful tool to investigate the dynamic response of the structure, allowing a preliminary structural assessment at the same time. The data recorded by the permanent dynamic structural health monitoring system installed on a masonry building, the Town Hall of Pizzoli in central Italy, are used to demonstrate the proposed model calibration strategy.

KEYWORDS

finite element calibration, metaoptimization, multicriterion updating, multiobjective updating, Plackett-Luce, rank aggregation

1 | INTRODUCTION

It is well known that an unresolved issue regarding the calibration of finite element models (FEMs), characterized by a large number of unknown parameters, concerns the reliability of the results of the optimization process. Although model updating is successfully used in vibration-based structural health monitoring (SHM),[1-7] its outcome usually represents an approximation of the real solution. In addition, there may be numerous parameter combinations that fall within the prefixed margins of error (*non uniqueness of the solution*). In a broader sense, when approaching inverse problems, the same methodology can lead to discrepant solutions, depending on the setting. A striking example is that of linear system identification, where a change in the order of the system can provide different values for modal parameters. The approach proposed in the present study tries to take advantage of the combinatorial selection of different solutions. Indeed, a synergic approach to information deriving from different methods, or from the same method undertaken in different ways, can lead to a unique reference result.

The aim of this study is therefore the definition of a strategy that can reduce the uncertainties of the solution provided by current model updating techniques and at the same time increase its reliability. This novel strategy is devised to be used in the calibration of reference numerical models to support existing monitoring systems of buildings. This is achieved by manipulating the combinations that are considered to be optimal according to different approaches, leading to the choice of a unique reference result. It is not the intention of the authors to affirm that the result is unique in a broad sense, but rather to demonstrate that, starting from multiple solutions, the strategy leads to a reference solution which respects certain optimal characteristics. In this regard, the concept of rank aggregation (RA) problem[8] is introduced. The goal of an RA problem is to define a ranking list among several ranking lists expressed by *voters*. The ranking lists arrange a certain number of *candidates* in a specific order. Thus, the aim of an RA problem is to find the best ranking list among all the possible permutations of the candidates' order. The RA problem is a classic problem in social choice literature[8] and has been applied to a wide variety of fields, that is, the rank of documents,[9] to assess the potential demand for electric vehicles,[10] to model electorates,[11] and so on. In recent years, the problem has also been explored by the computer science community,[12-14] in particular, it has been addressed with efficient Bayesian methods for inferring the parameters of a specific ranking model,[15] such as the Plackett-Luce (PL) model.[16-18] Inferring the parameters of the PL distribution is typically done using maximum likelihood estimation by means of the *minimization/maximization* (MM) algorithm.[19] However, the Bayesian inference has proven to be very accurate and highly scalable to large real-world problems.[20,21] Lately, the RA problem has been addressed by using evolutionary algorithms,[22] or other specific learners,[23] in the machine learning community. Here, the RA problem is dealt with by using a PL model to select the permutation of the candidates that maximizes the probability of being observed. In this regard, the candidates are supposed to be well-known optimization methods, as described in Section 2. In other words, this work implements a "ranking" strategy to obtain optimal results from several optimization algorithms, such as genetic algorithm (GA), particle swarm optimization (PSO), pattern search (PS), and simulated annealing (SA). In the application of the methodology, the default setting of the solvers[24] has been used to allow easy reproducibility of the work, without limitations to the generality of the methodology produced by the setting of the solvers or by its type. Metaheuristic algorithms are useful for dealing with problems characterized by nonsmooth and unknown cost functions (without a closed formulation). In addition, the calibration of very complex systems is often performed with these algorithms because of their ability to deal with problems characterized by a large number of parameters and uncertainties. These methods, however, present some disadvantages, mainly related to the low precision of the results. Thus, different trials in the calibration process may lead to different results in the values of the updated parameters. This is true for metaheuristic and for a large number of other algorithms that try to solve an inverse problem. In this regard, it is worth mentioning that to increase the accuracy of optimization, several improved versions of the aforementioned algorithms have been proposed in the literature. For example, the quantum-PSO (QPSO) was proposed by Sun et al[25] to introduce a quantum behavior of the swarms. This allows numerous disadvantages of the classical PSO to be overcome while maintaining all its advantages.[26] A noteworthy modified and efficient version of the QPSO is represented by the chaotic-PSO (CQPSO),[27] which adds chaotic sequences in the optimization process. However, the scope of this paper is to demonstrate the use of RA to obtain optimal results from several competing optimization techniques, either in their standard or enhanced versions, to reduce the discrepancy of the results in calibration procedures. The RA strategy helps in reducing this discrepancy by combining the outcomes of each algorithm and providing a learning phase. All this leads to a more reliable value of the parameters being updated thanks to the information exchanged between the solvers.

A further motive to use RA lies in its combining many different rank orderings on the same model parameters to produce "best" compromise orderings. This paper shows how to efficiently take any initial aggregated ordering, resulting from different optimization algorithms, and produce a maximally consistent locally optimal solution. Finally, as will be shown in the paper, the RA strategy can also be an optimal tool to allow multiobjective and multicriterion optimization very easily, maintaining at the same time a physical meaning, that is, the provided solution is the one that maximizes the probability of being observed and minimizes the variance of the results between different solvers.

In order to provide an experimental demonstration, the RA approach is applied to a real monitored building. The selected two-story masonry structure is the Town Hall of Pizzoli (AQ), which was affected by the recent 2016 Central Italy earthquake. In particular, the recorded main shocks are those occurred on August 24, 2016, October 26, 2016, and October 30, 2016. In fact, the Town Hall of Pizzoli is part of the network of strategic buildings monitored by the Seismic Observatory of Structures (OSS). It is worth underlining that, to the best of the authors' knowledge, this is the first study to undertake RA strategies to achieve the optimal selection of a calibrated model for monitored buildings.

The paper starts with a description of the combinatorial selection strategy (Section 2). Then, to test its effectiveness, the strategy is applied to well-known optimization problems, as well as to a purely numerical benchmark model (Section 3). The paper continues with an overview of the Town Hall building of Pizzoli, the seismic events that occurred in 2016 in central Italy, and the installed monitoring system. After the processing of the experimental data, the strategy is applied to the structure of the Town Hall (Section 4). Finally, the results of the study are reported and discussed (Section 5).

2 | RA PROBLEM IN THE OPTIMIZATION FRAMEWORK

The problem of selecting the best result among several optimal results can be reduced to a ranking problem in *learning to rank* theory.[9,28] Specifically, the RA problem[8] aims to find the best ranking list of I candidates of an item q (part of a total number of Q items) from several ranking lists provided by K voters. Among many models, the PL one has proved to be a very effective tool to solve the RA problem.[16] As K represents the number of voters (entities related to experimental quantities) and Q is the number of the items to be updated (i.e., unknown model parameters), a relation between these two numbers exists. In fact, K can be seen as a degree of restraint of the optimization, whereas Q represents the number of degrees of freedom of the problem. Thus, in order to obtain reliable results, as in any optimization problem, the number of experimental quantities, K, should be close to or greater than the number of the unknown parameters, Q. The greater the difference, the lower the risk of overfitting. An effective tool to increase this difference is represented by *global sensitivity methods*,[29] through which the number of items, Q, to be calibrated is reduced and restricted to the items that cause the main variability of the measurement predicted by the model (which is compared with experimental quantities). These methods[30] commonly outperform other standard methods of sensitivity analysis, such as those based on local estimators (e.g., gradient).

Instead, as regards the number of candidates, I, it is worth mentioning that its value is limited in the range 2–12. The lower bound is needed to obtain a synergistic optimization result (i.e., combining more than one solver), whereas the upper bound depends on the computational power of the machine being used. In particular, the number of candidates should not be greater than 12. This is due to the high number of permutations of the ranking lists that are generated, that is $I!$, which nowadays is difficult to be stored in any existing computer if I is greater than 12.

The PL distribution derives its name from independent works by Plackett (1975) and Luce (1959).[16] The Luce's axiom governs the choice probabilities of a population choosing an item from a subset of a set of items. The axiom states that the choice probability ratio between two items is independent of any other items in the set. Given a set of items and a set of choice probabilities, one item at a time out of the set is chosen, according to the choice probabilities. Such samples give a ranking of items, which can be considered as a sample from a distribution over all possible rankings. The form of such a distribution was first considered by Plackett in order to model probabilities in horse races and, combined with Luce's axiom, is easily extended to partial rankings. The PL model applies when each observation provides either a complete ranking of all items, or a partial ranking of some of the items, or a ranking of the top few items. In more detail, by means of this approach, each voter k gives a score $w_{k,i}$ to the ith candidate. The score represents the probability of picking the candidate i among the other candidates (Luce's axiom). In order to define who is the best candidate to be selected, it is necessary to follow some criteria. In this regard, the PL model aims to maximize the compound probability to observe some rankings or permutations of the candidates, assuming that both the voters and the candidates are independent. The total number of permutations is evaluated starting from the indices i, which identify each candidate. Given the total number of candidates, I, it is possible to build the vector of the permutation indices, $\boldsymbol{t} = 1,2,..,i,..,I$, which contains the positive natural numbers that go from 1 to I with step 1. The permutation matrix $\mathbf{C}$ containing all the P possible permutations is given by $\mathbf{C} = perms(\mathbf{t})$,[24] with $\mathbf{C} \in \mathbb{N}^{PxR}$, $R = I$ and $I!$.

To explain how RA works, we will use an analogy, comparing the RA to the teacher-led work of a class that has to solve an assignment. In teacher-led work, teachers help students to accomplish a specific project by providing explicit instructions, or explanations. The task given by the teachers actually represents the optimal solution that the class must achieve. In teacher-led work there is no competition in the classroom, but teachers help all the students to solve the assignment and to find the best solution accepted by everyone. In this type of problem, the teachers do not know the optimal solution of the work; they can just guide the students.

In this first phase of the teacher-led work, each student must solve the assignment independently. Once all the students have completed the assignment, based only on their individual skills, they will deliver it to the teachers. This first phase is equivalent to reaching the optimum for each single algorithm, according to the convergence criterion adopted.

If the task is extremely difficult, none of the students would be able to solve the assignment obtaining the 100% of the score; in other words, none of them would reach a satisfactory result. This first phase is depicted in Figure 1.

After collecting all the completed assignments, teachers evaluate them independently by giving a score to each student. At this point, the problem arises about the best ranking to be adopted. In fact, as teachers do not know the exact solution, they might disagree about the score to assign to the students. For this reason, teachers need to use a decision-making method that helps them to find a reference solution, represented by a ranking that classifies the assignments from the best to the worst. This second phase, as depicted in Figure 2, corresponds to the estimation of the score related to the difference between the experimental quantities and the numerical quantities provided by each algorithm.

Since teachers disagree about the classifications they have drawn up, they decide to question their own results. Therefore, they decide to analyze all the possible permutations of the assignments. In this way, a finite number of ranking lists is generated and, consequently, a finite number of possible solutions to the problem. The solution of the RA aims to determine which list sorts the assignments, and therefore the students, from the best to the worst. This third step (see Figure 3) corresponds to the calculation of the permutation matrix **C**, as described before.

2.1 | PL model to solve the RA problem in the optimization framework

Having defined the permutation matrix, **C**, for the pth permutation and for the kth voter, it is now possible to evaluate the probability of selecting a candidate instead of another one, having already selected a certain number of candidates:

$$f_{p,k} = \prod_{r=1}^{R} \frac{w_{k,C_{p,r}}}{\sum_{s=r}^{R} w_{k,C_{p,s}}}, \tag{1}$$

where $w_{k,Cp,r}$ is the weight that the voter k gives to the candidate $C_{p,r}$, that is, the rth candidate of the pth ranking obtained by permutation. Moreover, $R = I$ is the total number of candidates, and s is an auxiliary variable. Equation (1), which describes the PL model, can then be used to evaluate the probability observing a permutation set:

$$f_p = \prod_{k=1}^{K} \left(\prod_{r=1}^{R} \frac{w_{k,C_{p,r}}}{\sum_{s=r}^{R} w_{k,C_{p,s}}} \right), \tag{2}$$

The permutation that maximizes Equation (2) defines the best ranking list that should be selected, since it is related to the maximum probability of being observed (maximum likelihood). Indicating the selected ranking list with $a^* = C_{p^*,\forall r}$, a method (e.g., mean reciprocal rank) can be chosen to define the optimal value of the analyzed item, among all the candidates ranked as established by a^* (p^* is the index of the row of **C** related to the permutation that maximizes

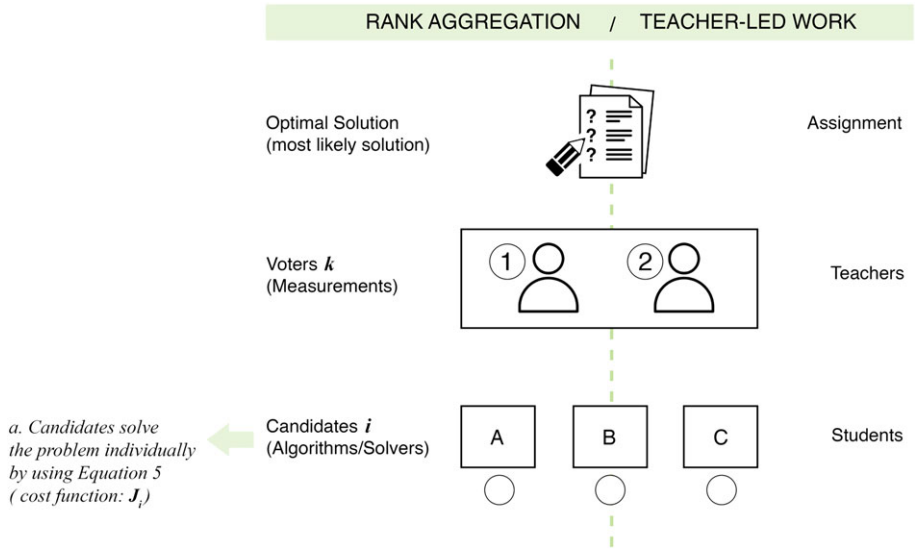

FIGURE 1 Teacher-led work

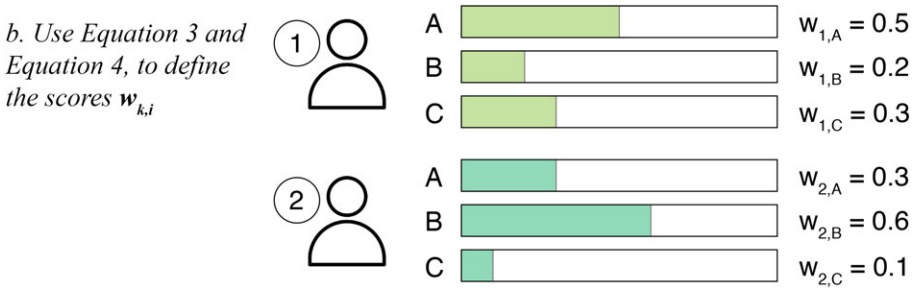

FIGURE 2 Teachers evaluate the assignments independently by giving a score to each student and thus defining the rankings

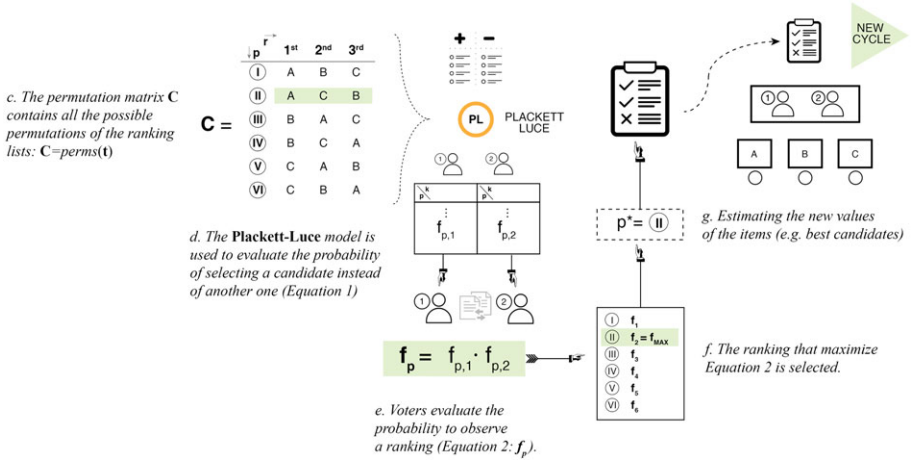

FIGURE 3 Teachers follow a Plackett-Luce model to propose a unique ranking of the assignments

Equation 2). For example, supposing we choose the first classified candidate, the optimal values of the analyzed items will be the ones related to the best candidate, according to the ranking list permuted as a^*. This means that the best candidate, i^*, is equal to $i^* = a_1^* = C_{p^*,1}$, and the optimal items are the ones related to the candidate i^*.

In this study, the items are represented by the parameters obtained from the different optimization solvers; thus, the candidates are chosen to be the optimization solvers, that is, GA,[31] PS,[32] PSO,[33] and SA.[34] For reproducibility reasons, the default setting of the solvers has been maintained.[24] In a more general framework, the candidates could be represented by one or more solvers with different settings. The voters are instead chosen to be the normalized scatters between the numerical and experimental measurements, but in the general case they can represent any objective. It is important to note that common problems in the calibration of engineering structures involve a minimization process. However, the RA is solved through a maximization process. For this reason, one needs to change the minimization process of each algorithm into a maximization process for the PL model. Thus, for each solver i, we can define a normalized scatter, $\beta_{k,i}$, between the kth numerical $z_{k,i}$, and the kth experimental, $z_{k,e}$, measurements as

$$\beta_{k,i} = \frac{\left|z_{k,\mathrm{e}} - z_{k,\mathrm{i}}\right|}{\left|z_{k,\mathrm{e}}\right| + 1}, \tag{3}$$

then the scores, $w_{k,i}$, are assumed to be calculated starting from the scatters, $\beta_{k,i}$, using the Gaussian function of Equation 4:

$$w_{k,i}^{*} = \exp\left[-\left(\frac{\beta_{k,i}}{\sigma_k}\right)^2\right], \tag{4a}$$

$$w_{k,i} = \frac{w^*_{k,i}}{\sum_{i=1}^{I} w^*_{k,i}}. \tag{4b}$$

In Equation (4a), σ_k is the standard deviation of the kth scatter among the solvers. It is important to note that Equation (4a) does not represent the probabilistic distribution of the scores but just the relationship that allows the minimization to be converted into a maximization problem. As a matter of fact, in the present study, the inference of the parameters of the probabilistic distribution of the scores is not undertaken. It is worth noting that $w_{k,i}$ in Equation (4) and $w_{k,C_{p,r}}$ in Equations (1) and (2) have the same meaning, as they represent the same quantity. More specifically, $w_{k,i}$ is a generic definition of the weight starting from Luce's axiom and the subscript, i, can take any nonnegative natural value. Instead, with $w_{k,C_{p,r}}$, the subscript $i = C_{p,r}$ denotes a generic candidate, i, listed in the pth ranking list, in the rth ranking position. Or in other words, $C_{p,r}$ is the value of i, contained in the pth row and rth column of the permutation matrix, $\mathbf{C}$. For example, referring to Figure 3, $C_{3,2} = i = \mathrm{A}$, $C_{4,1} = i = \mathrm{B}$, and so on.

To better explain the PL model, we will continue the analogy of the RA with the teacher-led work of a class. We are now in the fourth step of the RA problem. To decide which is the optimal ranking, the teachers decide to use a model of PL. With this model, each teacher calculates the probability of choosing one winning student instead of another, having already taken into account the score of the other students. At this stage each teacher will use the score given in the previous phase. In this way, the teachers can assign a value to each permutation of the rankings; these values correspond to the probability of observing a certain ranking rather than another, on the basis of the individual skills of the teachers. In fact, each teacher will obtain a result independently from the other teachers. This phase corresponds to the use of Equation (1), see Figure 3 for clarity.

Following the employment of the PL model, the teachers compare their results and decide to combine the probabilities to observe a winning ranking rather than another one. Since both the grading processes have been carried out independently, the teachers choose to multiply the probability values for each permutation, thus calculating the compound probability to observe a permutation rather than another one. In this way, a shared reference value of probability for each permutation is set. The teachers will determine which ranking permutation maximizes the probability to be observed, which is the most plausible ranking that orders the students (and therefore the assignments) from the best to the worst. This phase (see Figure 3 for clarity) corresponds to the application of Equation (2) and, consequently, to the determination of the ranking that orders the algorithms from the one who provides the "best" result to the "worst."

After obtaining a list that ranks the assignments in the most plausible way, the teachers will determine if the best assignment is just the one in first place or a combination of the results of each individual assignment. An example of combination is represented by the "mean reciprocal rank," which would correspond to a mean value of the results of each assignment, weighted according to the position occupied by each assignment in the most-plausible ranking. The type of method used to combine the outcomes of the calibration procedures will be strongly influenced by the user needs. If the optimization involves large-scale models, the most appropriate method (being the most efficient) is the one of the *best candidate* (i.e., the outcomes are provided by the candidate in first place). This is needed to obtain results in reasonable time. Instead, if the calibration refers to small models, or high computational power is available, a weighting scheme of the outcomes should be considered to increase precision. A well-known and widely used weighting scheme in ranking theory is *mean reciprocal rank*. However, several other methods exist, such as *mean average precision*. Mean reciprocal rank is more appropriate when one trusts the outcomes of the first three and four classified candidates, as the weight is proportional to the inverse of the position of the candidate, r. Instead, mean average precision weights the candidate's outcomes in a smoother way, assigning importance even to the lowest ranked candidates. In general, in the information retrieval field, these weighting schemes are called *evaluation measures*. Details on their selection and use can be found in the literature.[35]

This phase corresponds to the calculation of the "mean reciprocal rank" value of each parameter updated by the various algorithms. The parameters that are defined as optimal will correspond to the mean of the parameters of each single algorithm; the mean is weighted according to the position of the solvers/students in the most plausible ranking. Alternatively, the optimal parameters can be chosen as the parameters associated with the algorithm in first place in the most likely ranking.

In this last phase, the teachers show the students a single reference assignment, explaining to them that it is the task that most likely corresponds to the optimal solution, and ask them to solve the same problem again. Therefore, the students have to do the assignment again, but this time being aware that the most plausible solution, up to that point, is the one given by the teachers. The procedure can continue until all the students (i.e., the algorithms) reach a common

agreement, that is a common reference solution. The optimal result will not be the best in the broad sense (it does not necessarily correspond to a score of 100%), but it will rather be the most likely result, which at the same time maximizes the agreement between the different students. In this way, the whole class will reach a common solution.

This last phase (see Figure 3) corresponds to identifying the parameters (object of the calibration) that satisfy two conditions: (a) they are associated to the most plausible ranking list, in a sense that this list has the maximum probability of being observed (maximum likelihood); (b) their values maximize the correspondence of the results obtained by the different algorithms (minimum variance). A pseudocode of the proposed selection algorithm is reported in Table 1.

3 | NUMERICAL TESTS

3.1 | Optimization of test functions

To assess the effectiveness of the proposed selection strategy, the RA problem is solved with the PL model applied recursively to a set of well-known optimization test functions[36] by choosing the candidate classified first by the selected permutation. The chosen parameters are thus imposed as the initial condition for the next optimization (PS and SA), or as an individual (GA) or a swarm component (PSO). Among a vast number of test functions existing in the literature, it was decided to use six of them to test the strategy. The testing functions used in this study are shown in Figure 4, and they are Rosenbrock's function, Levi's function n.13, Eggholder function, Easom's function, Bukin's function n.6, and Cross-leg table function, with the optimum shifted to $x_1 = 1$, $x_2 = 1$ (see Figure 4 for clarity). Although the first two functions are relatively simple problems, the last two are considered nearly impossible to minimize.[37] All the selected test functions are in two dimensions in order to give a visual representation.

The experimental measurements in this example are set to exactly correspond to the global minima of the functions, so that $K = 1$, $I = 4$, and the number of items (i.e., the parameters) is two, x_1 and x_2. For each test, Table 2 reports the experimental measurements (i.e., the global minimum) and the true values of the parameters with the respective searching space. For the optimization tests, the objective function of each solver i is the normalized scatter, $\beta_{k,i}$, between the kth numerical $z_{k,i}$, and the kth experimental, $z_{k,e}$, measurement. To compare the results of the optimization, a first study was performed in the absence of the PL model. For each test function, 1,000 trials with random starting points were evaluated. These results, in terms of parameter values, are reported in Figure 5, where only the first 50 trials are shown, for brevity's sake. Subsequently, the optimization tests were repeated in the same conditions by introducing the PL model. The results of the optimizations obtained with the PL are reported in Figure 6. The numerical results in terms of efficiency (i.e., number of function evaluations), accuracy (i.e., average normalized scatter between the real and

TABLE 1 Pseudocode of the selection algorithm involving the PL model

Having assumed *I* candidates (i.e., solver setups) and *K* voters (i.e., objectives of the optimization) to calibrate *Q* items (i.e., model parameters), the following procedure applies:
A. Initialize the values for different items (i.e., model parameters)
a. Set each candidate (i.e., solver) and perform an independent optimization with an assumed convergence criterion and a desired objective function, for example, Equation (5).
b. Use the outcomes of each optimization (i.e., model predictions) and the available experimental quantities (i.e., measured quantities) to estimate the weights with Equations (4) based on the assumed objectives (e.g., Equation 3).
c. Calculate the permutation matrix of the rankings, $\mathbf{C} = \text{perms}(\mathbf{t})$, where $\boldsymbol{t} = 1,2,..,i,..,I$ with Step 1.
d. Evaluate the probability of selecting a candidate (solver) instead of another one with Equation (1).
e. Evaluate the probability of observing a ranking from Equation (2).
f. Select the ranking that maximizes Equation (2).
g. Employ a method for estimating the new values of the items (i.e., model parameters), for example, best candidate, mean reciprocal rank, and mean average precision as described over Figure 3.
B. Start again, performing A in a recursive way up to convergence, that is until the variance of the values of the items (i.e., model parameters) calculated over all the candidates (i.e., solvers) is lower than a chosen tolerance.

Abbreviation PL, Plackett-Luce.

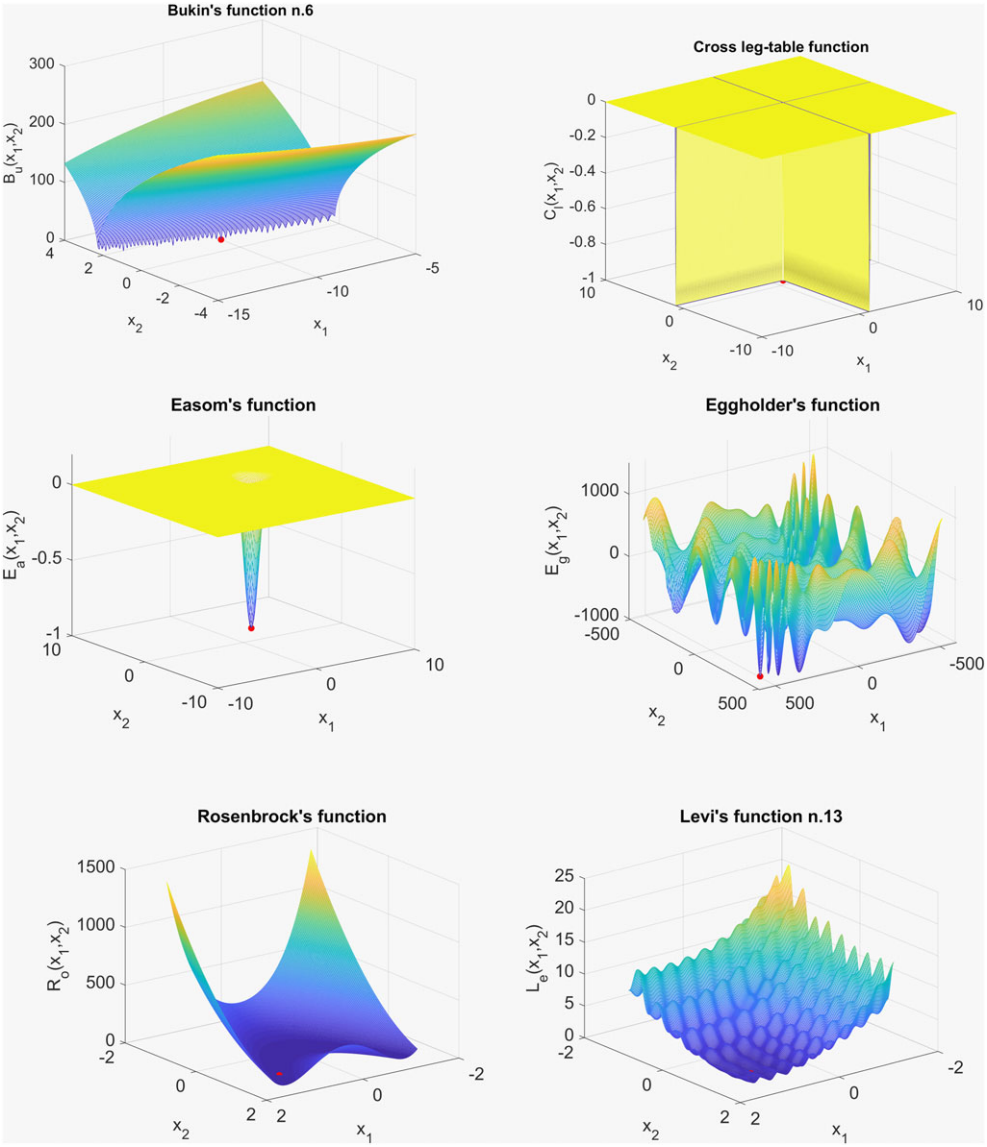

FIGURE 4 Optimization test functions. The global minimum is depicted by the dot

TABLE 2 Optimization tests data

Test	$z_{1,e}$	$x_1, x_2\|_{true}$	$x_1, x_2\|_{min}$	$x_1, x_2\|_{max}$
Rosenbrock	0	1, 1	−10, −10	10, 10
Levi	0	1, 1	−10, −10	10, 10
Eggholder	−959.6407	512, 404.2319	−512, −512	512, 512
Easom	−1	π, π	−100, −100	100, 100
Bukin	0	−10, 1	−15, −3	−5, 3
Cross-leg table	−1	1, 1	−10, −10	10, 10

the best values of the parameters found by the solvers), and precision (i.e., standard deviation of the normalized scatter between the real and the best values of the parameters found by the solvers) are instead reported in Tables 3–5, respectively. In these tables, the results, with and without the use of the PL model, are shown. Specifically, when using the PL model, in addition to the results of each solver, the most likely result among the solvers, for each trial is also obtained. This led to 1,000 additional results from the trials. The column PL in Tables 3–5 contains the efficiency, accuracy, and

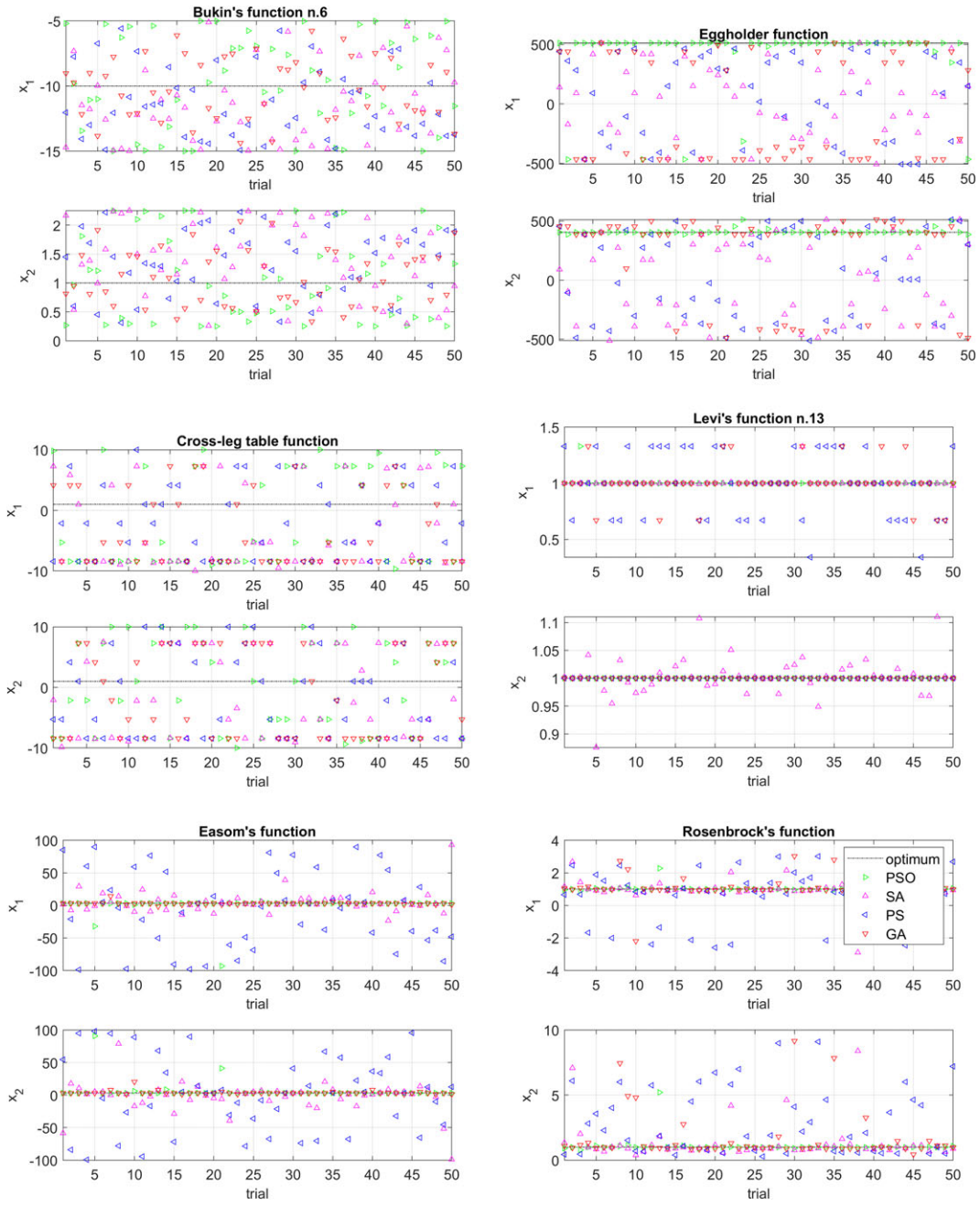

FIGURE 5 Test results without PL model: values of the parameters to be optimized. GA, genetic algorithm; PL, Plackett-Luce; PS, pattern search; PSO, particle swarm optimization; SA, simulated annealing

precision, respectively, for these 1,000 additional results, which are only provided in the case of optimization performed with the PL model. Thus, in Table 3, the column PL contains the sum of the values of the other columns, whereas for Tables 4 and 5, the column PL does not necessarily contain the "best" results but rather the accuracy and precision referring to the most likely results, that is the ones that minimize the discrepancies between the values obtained with different solvers, in accordance with the solution of the RA problem. In fact, the available experimental quantities commonly refer to a sample of all available data (i.e., population). In this situation, a very accurate matching of experimental results may hide overfitting problems (i.e., the model accurately reproduces the sample but fails to represent the population), mainly caused by inappropriate settings of the model parameters. For example, this can also be deduced from Figure 8, where quite accurate results in terms of modal data are obtained for inappropriate values of model parameters.

From Figures 5 and 6 and Tables 3–5 it is possible to note that the use of PL improves the accuracy and the precision of the calibration and, consequently, leads to more reliable results, thanks to the information that each solver takes from

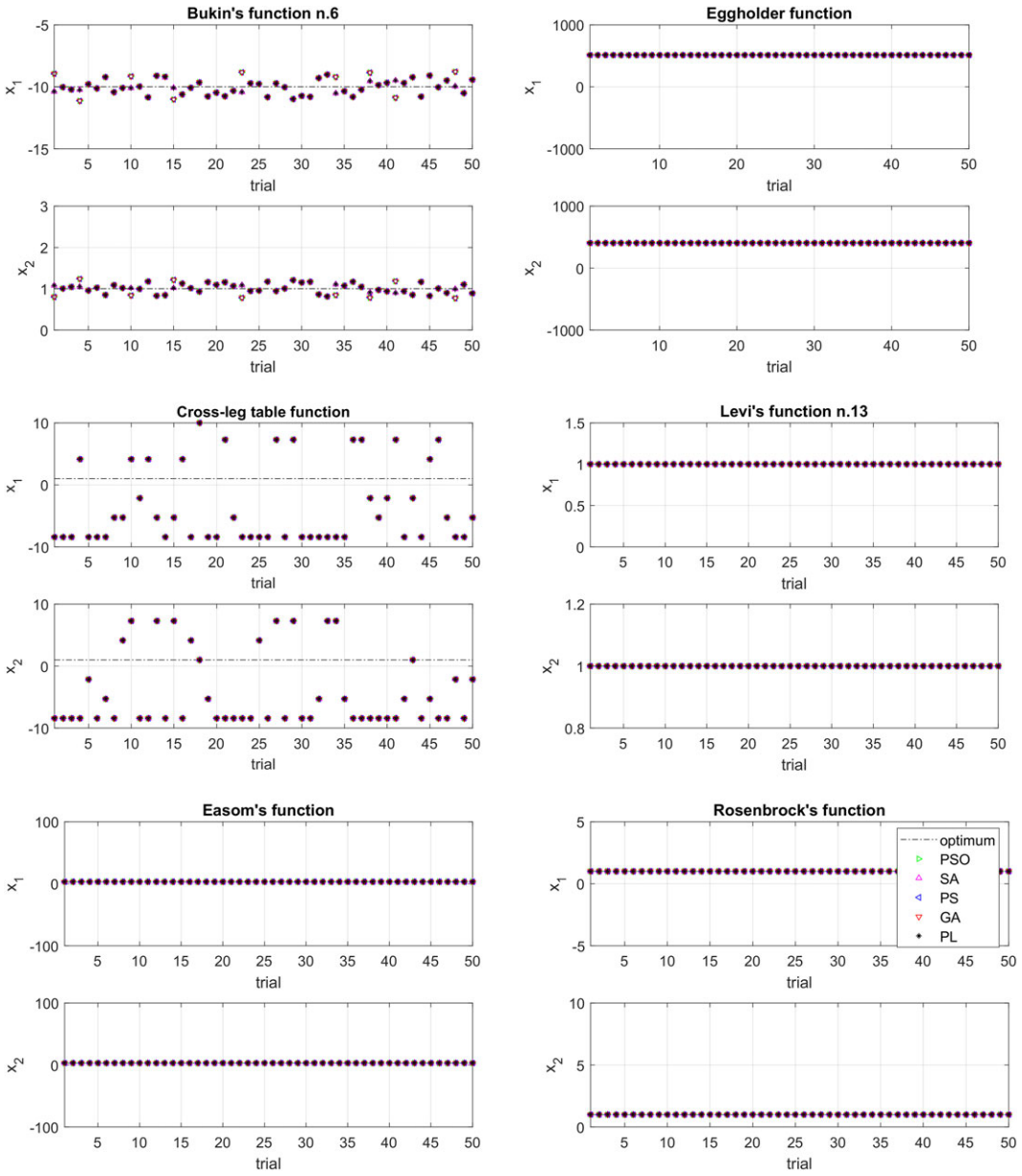

FIGURE 6 Test results with PL model: values of the parameters to be optimized. GA, genetic algorithm; PL, Plackett-Luce; PS, pattern search; PSO, particle swarm optimization; SA, simulated annealing

the others, although the efficiency decreases. However, a parallel session can reestablish the efficiency (in terms of computational time) to produce values comparable with those of a single solver.

3.2 | Benchmark FEM

In this subsection the proposed selection strategy is applied to a simple FEM, reported in Figure 7. The FEM is a linear elastic cantilever beam that implements the Timoshenko beam theory. It is discretized in three homogeneous portions of 1 m length, each discretized with 10 finite elements (see Figure 7 for clarity). The cross section is a square section of 0.1×0.1 m. The Young's moduli, E, the densities, ρ, and Poisson ratios, υ, are reported in Figure 7. The best values of the objective function, J_i, of each solver i are also reported in Figure 7. J_i is assumed to be

$$J_i = \frac{1}{K}\sum_{k=1}^{K}\left(z_{k,e} - z_{k,i}\right)^2, \tag{5}$$

TABLE 3 Efficiency (number of function evaluations); average of 1,000 trials

Test	Particle swarm optimization (PSO)	Simulated annealing (SA)	Pattern search (PS)	Genetic algorithm (GA)	Plackett-Luce (PL)
Without PL					
Rosenbrock	2,488	2,074	672	9,580	
Levi	1,094	1,858	202	3,919	
Eggholder	1,077	1,955	251	5,630	
Easom	1,198	1,054	103	3,713	
Bukin	2,129	1,823	132	5,661	
Cross l-t	2,550	1,786	187	6,026	
With PL					
Rosenbrock	3,989	4,335	1,178	16,044	25,546
Levi	1,517	2,870	283	6,476	11,146
Eggholder	1,857	3,572	377	9,712	15,518
Easom	1,715	2,172	190	6,098	10,175
Bukin[a]	4,851	9,286	598	21,538	36,273
Cross l-t[a]	19,157	37,761	2,903	99,271	159,092

[a]Optimization stopped for a tolerance of the objective function equal to 1E-2 instead of the default value 1E-6.

TABLE 4 Accuracy (%); average of 1,000 trials

Test	Particle swarm optimization (PSO)	Simulated annealing (SA)	Pattern search (PS)	Genetic algorithm (GA)	Plackett-Luce (PL)
Without PL					
Rosenbrock	6.46e0	4.87e1	1.94e2	5.81e1	
Levi	1.65e-1	1.57e0	9.74e0	5.95e0	
Eggholder	1.70e1	9.97e1	9.85e1	7.27e1	
Easom	6.79e1	3.68e2	1.37e3	4.12e1	
Bukin	4.72e1	4.67e1	3.94e1	3.56e1	
Cross l-t	7.43e2	6.84e2	5.98e2	6.77e2	
With PL					
Rosenbrock	5.96e-2	6.63e-2	6.38e-2	3.60e-2	3.20e-2
Levi	3.06e-4	1.24e-3	1.86e-4	1.94e-4	1.63e-4
Eggholder	1.47e-5	3.05e-5	1.17e-5	1.15e-5	1.16e-5
Easom	2.60e-4	2.72e-4	2.62e-4	1.05e-4	1.04e-4
Bukin[a]	8.78e0	6.79e0	8.78e0	8.78e0	6.79e0
Cross l-t[a]	7.14e2	7.14e2	7.14e2	7.14e2	7.14e2

[a]Optimization stopped at a tolerance of the objective function equal to 1E-2 instead of the default value 1E-6.

where $z_{k,i}$ is the kth numerical measurement related to the ith solver, whereas $z_{k,e}$ is the kth experimental measurement. For this benchmark problem, the number of experimental measurements is $K = 4$, namely, the first two frequencies, f_1 and f_2, and the related ideal Modal Assurance Criterion (MAC) (two unitary values) between the experimental and numerical modal shapes. The number of solvers is still $I = 4$. The items are instead three, namely, the number of Young's moduli, E, of the FEM.

The acceleration is recorded at two points of the model, that is the top point and the point at 1/3 of the total length (3 m). Clearly, a reliable optimization process should not involve too many parameters (e.g., Young's moduli) with

TABLE 5 Precision (%); average of 1,000 trials

Test	Particle swarm optimization (PSO)	Simulated annealing (SA)	Pattern search (PS)	Genetic algorithm (GA)	Plackett-Luce (PL)
Without PL					
Rosenbrock	2.89e1	9.81e1	1.80e2	1.07e2	
Levi	1.64e0	2.52e0	8.96e0	8.82e0	
Eggholder	3.64e1	4.70e1	5.55e1	6.19e1	
Easom	3.32e2	4.99e2	8.64e2	1.84e2	
Bukin	2.60e1	2.61e1	2.37e1	2.17e1	
Cross l-t	1.72e2	1.94e2	1.95e2	1.85e2	
With PL					
Rosenbrock	4.55e-2	4.88e-2	4.69e-2	3.96e-2	3.57e-2
Levi	5.74e-4	7.06e-3	1.51e-4	2.49e-4	2.01e-4
Eggholder	5.45e-5	1.20e-4	6.67e-8	1.18e-6	3.46e-6
Easom	4.24e-4	4.58e-4	4.06e-4	1.12e-4	1.10e-4
Bukin[a]	5.14e0	4.35e0	5.14e0	5.14e0	4.35e0
Cross l-t[a]	1.81e2	1.81e2	1.81e2	1.81e2	1.81e2

[a]Optimization stopped at a tolerance of the objective function equal to 1E-2 instead of the default value 1E-6 for time reasons.

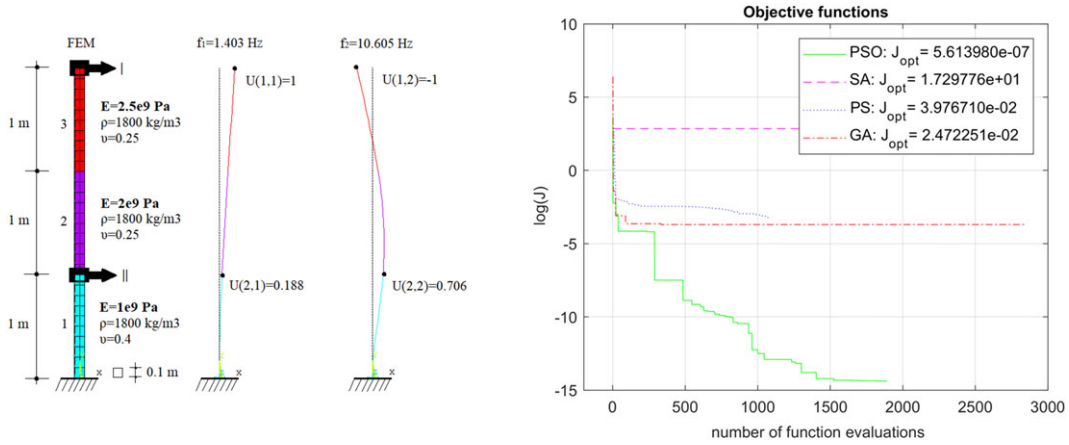

FIGURE 7 The FE model with the modes used in the calibration, and the objective functions of the solvers. FE, finite element model; GA, genetic algorithm; PS, pattern search; PSO, particle swarm optimization; SA, simulated annealing

respect to the number of available experimental data (e.g., number of modes). This is due to the risk of nonoptimal solutions in the broadest sense, that is solutions that satisfy the experimental data, but with nonphysical values of the calibration parameters. However, in order to consider some uncertainty in the calibration process, it is supposed that the experimental response of the point at 2/3 of the beam length is unknown. This leads to difficulty in finding the values of the Young's modulus of the second and third parts of the model (see Figure 7). The values taken as experimental measurements, together with the true values of the parameters and their searching space, are reported in Tables 6 and 7.

The optimization process was set to start from the values in the middle of the searching space. Finally, the scores are assumed to be in accordance with Equations (3) and (4). In this benchmark problem, the optimization was first performed without the PL model. The resulting best values of the objective functions for this situation are reported in Figure 7.

The results in terms of frequency and Young's modulus with and without the PL model are instead represented in Figures 8 and 9, respectively, whereas the exact numerical values of the results are reported in Table 8. For the benchmark model, the PL selection was able to reduce the uncertainties of the results, increasing the reliability of the

TABLE 6 FE benchmark model data: simulated experimental frequencies and MAC

k	$z_{k,e}$
1	1.403 (Hz)
2	10.605 (Hz)
3	1
4	1

Abbreviation: FE, finite element.

TABLE 7 FE benchmark model data: given expected true Young's moduli and boundaries for the optimization

q	$E_q\|_{true}$ (Pa)	$E_q\|_{min}$ (Pa)	$E_q\|_{max}$ (Pa)
1	1e9	1e8	10e9
2	2e9	1e8	10e9
3	2.5e9	1e8	10e9

Abbreviation: FE, finite element.

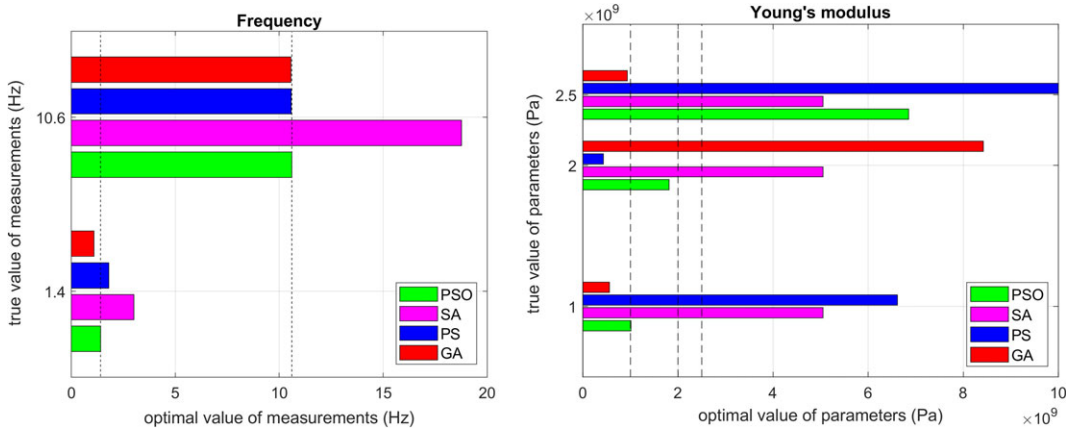

FIGURE 8 Results of the calibration. Modal frequencies (left) and Young's moduli (right) without PL model. GA, genetic algorithm; PL, Plackett-Luce; PS, pattern search; PSO, particle swarm optimization; SA, simulated annealing

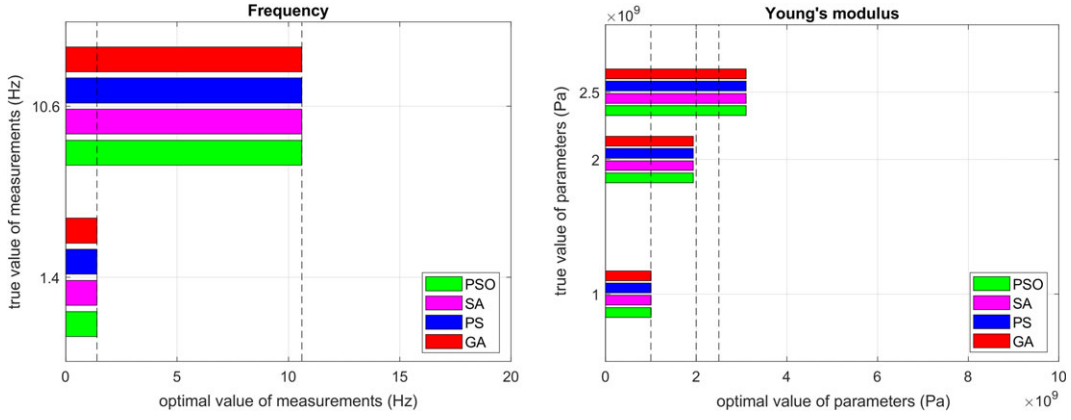

FIGURE 9 Results of the calibration. Modal frequencies (left) and Young's moduli (right) with PL model. GA, genetic algorithm; PL, Plackett-Luce; PS, pattern search; PSO, particle swarm optimization; SA, simulated annealing

TABLE 8 Numerical values found by the calibrations

Quantity	True value		PSO		SA		PS		GA		PL	
f_1 f_2 (Hz)	1.4	10.61	1.4	10.6	3.0	18.77	1.8	10.58	1.09	10.56	1.4	10.6
MAC	1	0.49	1	0.49	1	0.49	1	0.51	0.98	0.63	1	0.49
	0.49	1	0.49	1	0.45	1	0.56	0.99	0.62	0.98	0.47	1
E_1 (Pa)	1.000e9		1.008e9		5.049e9		6.616e9		0.557e9		1.002e9	
E_2 (Pa)	2.000e9		1.814e9		5.049e9		0.429e9		8.423e9		1.938e9	
E_3 (Pa)	2.500e9		6.852e9		5.049e9		9.999e9		0.935e9		3.105e9	

Abbreviations: GA, genetic algorithm; PL, Plackett-Luce; PS, pattern search; PSO, particle swarm optimization; SA, simulated annealing.

solution. As can be noted from Figure 9, the third Young's modulus is not satisfactorily replicated. This is due to the low sensitivity of the model with respect to that parameter. In fact, the middle portion of the model drives the upper one. In addition, it is possible to see that a small error affects the second Young's modulus. The influence of this small error on the total cost is covered by a value of E_3 very different from the true one. This is the same problem that affects the optimization in absence of the PL model, but, as can be noted by comparing Figures 8 and 9, the RA strategy was able to reduce the error, obtaining a more consistent result in terms of Young's moduli in the presence of lack of data (e.g., acceleration response at 2 m from the base).

4 | THE TOWN HALL IN PIZZOLI

Having established that the PL model can help increasing the reliability of the optimization, the strategy described in Section 2 is now applied to a real case study.

The aim is to establish a numerical FEM in support of the existing monitoring system installed on the Town Hall building of Pizzoli. Once updated, the FEM can be used to simulate the linear dynamic response of the building and, by defining some warning indicators, to assess the presence of pathological behaviors of the structure. This section starts with an overview of the monitored stone masonry building to introduce the critical condition in which the building of the Town Hall of Pizzoli found itself.

4.1 | Description of the building

The Town Hall of Pizzoli is a two-story stone masonry building located northwest of the city of L'Aquila (Abruzzo), which is about 15 km away. The Town Hall, overlooking one of the main piazzas of the town, was built around 1920, and it formerly hosted a school (see Figure 10). The building presents a u-shaped regular plan, mainly distributed along one direction, and its elevations are characterized by regular openings. The building has three levels above the ground (the raised ground floor, the first floor, and the under-roof floor) and a basement (see Figure 11 for clarity). The total area is about 770 m^2, whereas the volume is about 5,000 m^3. The main dimensions of the building are reported in Figure 11. Previous investigations have highlighted that the Town Hall presents mixed masonry consisting of

FIGURE 10 A historical postcard showing the Town Hall (on the left); a current view of the building (on the right)

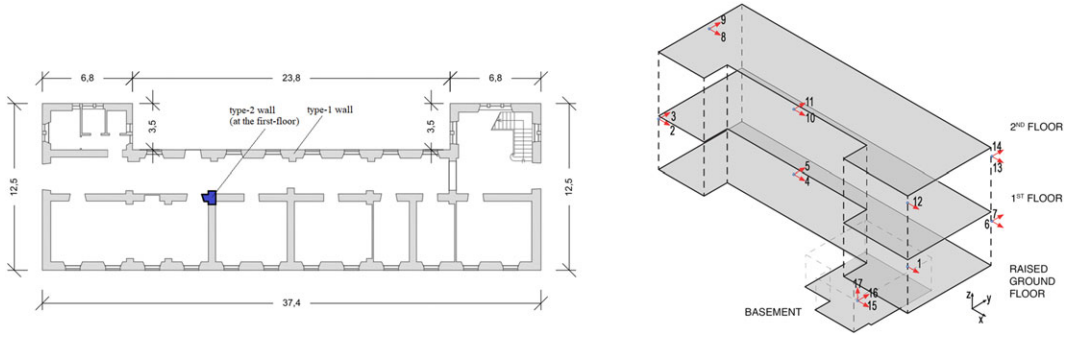

FIGURE 11 The plan of the raised floor reporting the main dimensions (in meters; left), scheme of the accelerometers installed on the Town Hall of Pizzoli (AQ; right)

unsquared stone blocks, alternated with solid bricks strips. Over the years, the Town Hall has been subjected to various transformations.

The original wooden roof was replaced with a reinforced concrete roofing system. Then an external elevator was attached to the north façade, and stairs in reinforced concrete were added. The Town Hall of Pizzoli is part of the network of buildings monitored by the OSS.[38] The seismic acquisition system installed in this building was in operation during the sequence that struck central Italy in 2016.

4.2 | Seismic records

The OSS permanent monitoring system allowed the recording of the seismic response of the Pizzoli Town Hall before and during the recent earthquakes that struck central Italy in August–October 2016. The main shocks of this seismic swarm occurred on August 8, 2016, and October 26–30, 2016. Figure 12 reports the seismic swarm dated October 30, 2016; the star markers identify the epicenters of the main shocks that exceeded 5.0 ML. In the same figure, the main features of the recorded seismic data are summarized: date and time of occurrence, geographical coordinates of the epicenter, and Richter magnitude (ML).

4.3 | Monitoring system

The Town Hall of Pizzoli belongs to the network of strategic buildings monitored by the OSS, which is also responsible for the installed monitoring system. The OSS is a nationwide network founded in the 1990s by the Italian Department of Civil Protection. The aim of this network is to permanently monitor several strategic Italian buildings.[38-40] Indeed, considering the intense seismic activity affecting the Italian territory and the earthquakes that periodically occur (e.g., Umbria-Marche 1997; L'Aquila 2009; Emilia Romagna 2012; Central Italy 2016), studies and investigations on the seismic behavior of civil buildings are increasingly important. The buildings monitored by the OSS can be divided

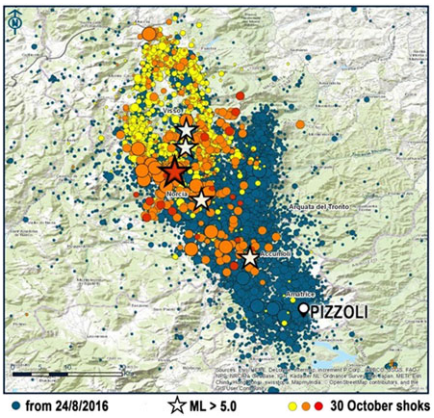

Date	Time	Lat.	Lon.	ML
24/08/2016	01:36	42.7	13.23	6
07/09/2016	03:29	42.68	13.29	1.6
26/10/2016	17:10	42.88	13.13	5.4
26/10/2016	19:10	42.91	13.13	5.9
30/10/2016	06:40	42.83	13.11	6.5

FIGURE 12 Seismic data from INGV

into two groups: the first group includes 300 buildings monitored by a simplified monitoring system composed of seven accelerometers; the second group, instead, comprises 105 strategic buildings (mainly schools, hospitals and city halls), 10 bridges, and a few dams all equipped with a dynamic permanent monitoring system of about 16–32 accelerometers each. The dynamic monitoring system installed on the Pizzoli Town Hall is composed of 17 accelerometers. A set of three uniaxial accelerometers is located in the basement at ground level, oriented along the main directions X, Y, and Z (sensor number 15-16-17). Three biaxial accelerometers in X and Y directions (2-3; 4-5; 6-7), and a uniaxial in X direction (1), are located on the raised ground floor. The same number of sensors is assigned also on the first and under-roof floors (8-9; 10-11; 12; 13-14), as can be noted by Figure 11.

4.4 | Modal identification

This subsection reports the results of a modal identification of the stone masonry structure of Pizzoli's Town Hall,[34] which relies on the acceleration data recorded by the OSS.[38,41] For its extensive use and proven validity, the identification method adopted for the case study is the Subspace State-Space System Identification implemented in the N4SID algorithm.[42,43]

Since the aim of the present study is to develop a linear FEM in support of the monitoring system, the structure is identified from the records of July 2015, thus acquired before the seismic events in central Italy. However, it is worth noting that, at that time, the structure had already been affected by the earthquake of L'Aquila (2009). For the case study, the state-space model is estimated by varying the order of the system between 2 to 42 (order step equal to 2) in an input–output time domain identification. Channels 1–14 are used as output signals, whereas the three channels at the base of the building (15–17) are used as input signals (see Figure 11 for clarity). The modes are accepted only if the value of the estimated damping is within the limits 0.9–5.5%. Then the optimal order, $n = 28$, is selected through clustering operations in the frequency-damping plane. The identified values of the damping ratio, ζ, frequency, f, and modal shapes, $\mathbf{U}$, are reported in Table 9 for the first four modes. The experimental frequencies and modal shapes are used to calibrate the FEM of the structure.

4.5 | FE modeling

For the FE modelling of the Town Hall building of Pizzoli (Figure 13), two element types are used: a two-node beam element, which implements the Timoshenko theory, is used for the reinforced concrete beams and the steel beams of the elevator frame, and a four-node thick shell element with bilinear shape functions is used for the slabs and the masonry walls. A spring element is also used to model the uncertainties of the geometry and materials below the mezzanine floor (boundary conditions). The numerical model has 52,369 nodes for a total number of 53,919 elements. The average dimension of each element is about 0.25 m for both the shell and beam elements. For the raised ground floor, the average thickness of the external and internal walls can be set equal to 0.63 and 0.54 m, whereas for the first floor, the same average quantities are 0.60 and 0.50 m, respectively. The actual values used for the simulation are set in accordance with the data obtained from a direct survey. The thickness of the portion of the walls located below the windows is 0.41 m (except for the area in which the stairs are situated, for which the thickness is equal to that of the wall above), whereas the thickness of the infill walls is set at 0.1 m. The cross-section dimensions are as follows: a rectangular section of 0.35 × 0.30 m (depth × width) for the reinforced concrete beams and a square hollow steel beam section of 0.18 × 0.18 m, 0.004 m thick, for the elevator frame. The stairs are modelled as 0.20-m-thick plate. The equivalent thicknesses of the raised ground, first, under-roof floor, and the roof plate are assumed to be 0.22, 0.22, 0.16, and 0.22 m, respectively, in accordance with the inspection. Other geometric quantities are reported in Table 10, whereas Table 11 contains the values initially assumed for the elastic parameters of the materials, in accordance with the data available from the survey. The static displacements field due to gravity loads is then illustrated in Figure 13.

4.6 | Selection of the best candidate

In this subsection, the strategy for the calibration and the selection of the best candidate, illustrated in Section 2, is employed. For the FEM updating of the Pizzoli Town Hall, the objective functions of the $I = 4$ solvers are described

TABLE 9 Identified damping ratio, frequency, and modal shape from the records of July 2015 (first four modes)

Mode			1	2	3	4
ζ (%)			1.08	1.80	2.00	1.25
f (Hz)			4.827	5.835	7.013	9.260
U	Channel	Direction				
	1	X	0.0434	0.0592	−0.2867	−0.2591
	2	X	−0.0642	0.1013	−0.2825	0.4018
	3	Y	−0.3629	−0.3631	0.0544	−0.6132
	4	X	0.0079	0.0490	−0.2883	−0.0055
	5	Y	−0.3238	0.0627	−0.0638	0.4341
	6	X	−0.0311	−0.0910	−0.3661	0.1966
	7	Y	−0.2100	0.3681	−0.0095	−0.4154
	8	X	−0.0148	0.0121	−0.6200	0.1297
	9	Y	−0.5450	−0.4952	−0.0205	−0.7729
	10	X	0.0292	0.1563	−0.8433	0.0124
	11	Y	−1	0.2786	−0.2679	0.9469
	12	X	0.1594	0.1367	−0.8293	−0.7372
	13	X	−0.1204	−0.1424	−1	0.4308
	14	Y	−0.5770	1	−0.0591	−1

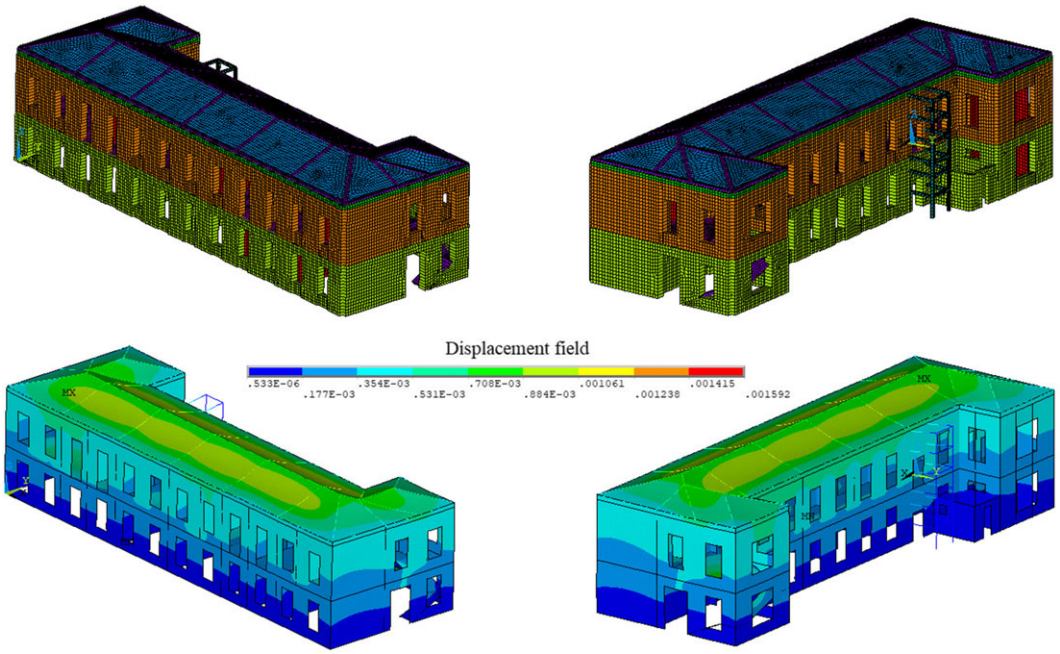

FIGURE 13 Finite element (FE) model of the Town Hall building of Pizzoli and linear elastic FE analysis considering gravity loads (displacement field in meters)

by Equation (5), where $K = 8$ is the number of normalized scatters between the experimental and numerical frequencies and the number of ideal MAC between the experimental and numerical modal shapes. The scores are still modelled as described by Equations (3) and 4. In this first updating of the structure, we are interested in the soil–structure interaction. In fact, although for the superstructure the availability of data from direct survey allows a certain degree of confidence in the values assumed for the geometry and materials, for the portion of the structure connected to the ground, some uncertainties still remain. The main uncertainty is related to the shape of the foundation and, thus, to the depth of the portion of the building under the raised ground floor, particularly for the inner walls of the building (the depth is in the range of 0.4–0.8 m for the external walls). To model these uncertainties, two spring systems with different stiffnesses are imposed at the raised floor level, in the two horizontal directions (X and Y). In the vertical

TABLE 10 Geometric quantities, between the center of the cross section of the component of the FE model (Town Hall of Pizzoli)

Description of the component	Dimension (m)
Height of the ground raised floor walls	4.00
Height of the first floor walls	4.50
Upper height of the windows	3.30
Bottom height of the windows	0.85
Average width of the windows	1.20
Height of external doors	3.30
Average width of external doors	1.95
Upper height of the internal windows	1.85
Bottom height of the internal windows	0.85
Average height of internal doors	2.40
Average width of internal doors	1.15
Height of the first stairway landing	1.40
Height of the second stairway landing	2.70
Width of the stairway landings	1.30
Height of the under-roof floor walls	0.35
Height of the top truss of the roof	1.50
Height of the attached masonry room	2.60
Width of the attached masonry room: X/Y	2.95/3.50
Height of the 1st, 2nd, 4th, 5th, and 6th "interstory" of the elevator frame	1.50
Height of the 3rd "interstory" of the elevator frame	1.00
Width of the elevator frame: X/Y	1.90/2.30
Height of the elevator doors and the attached masonry room door	2.20

Abbreviation: FE, finite element.

TABLE 11 Initial linear elastic parameters of the FE model (Town Hall of Pizzoli)

Id.	Description	E (Pa)	ρ (kg/m3)	υ
1	Steel	210e9	7,850	0.27
2	Concrete	30e9	2,500	0.25
3	Perforated brick masonry (infill walls)	4.5e9	1,500	0.30
4	Hollow block floor (roof)	13e9	1,914	0.30
5	Hollow block floor with steel beam (under-roof)	25e9	2,063	0.30
6	Full brick masonry (type-2 and under-roof walls)	1.5e9	1,800	0.30
7	Stone masonry (type-1 first floor)	2.8e9[a]	2,200	0.30
8	Hollow block floor with steel beam (raised ground and first floor)	25e9	2,082	0.30
9	Stone masonry (type-1 raised ground floor)	2.8e9[a]	2,200	0.30
10	Spring in Y, imposed at the raised ground floor level	5e7[a]	K_Y (N/m)	
11	Spring in X, imposed at the raised ground floor level	5e7[a]	K_X (N/m)	

Abbreviation: FE, finite element.

[a]Values updated during the calibration (see Section 4.6).

direction, Z, a rigid constraint is assumed. Because many uncertainties are present in the Young's modulus value of the stone masonry as well, in this first updating, the parameters of the optimization are assumed to be the Young's moduli of the raised ground and first floor walls of the building, as well as the stiffness of the two spring systems. This choice

TABLE 12 FE model updating: experimental frequencies and MAC

k	$z_{k,e}$
1	4.827 (Hz)
2	5.835 (Hz)
3	7.013 (Hz)
4	9.260 (Hz)
5	1
6	1
7	1
8	1

Abbreviation: FE, finite element.

TABLE 13 FE model updating data: starting values and boundaries for the optimization

q	Starting values	Lower bound	Upper bound
1. E_7	2.8e9 (Pa)	1.2e9 (Pa)	5e9 (Pa)
2. E_9	2.8e9 (Pa)	1.2e9 (Pa)	5e9 (Pa)
3. K_Y	5e7 (N/m)	1e7 (N/m)	9e7 (N/m)
4. K_X	5e7 (N/m)	1e7 (N/m)	9e7 (N/m)

Abbreviation: FE, finite element.

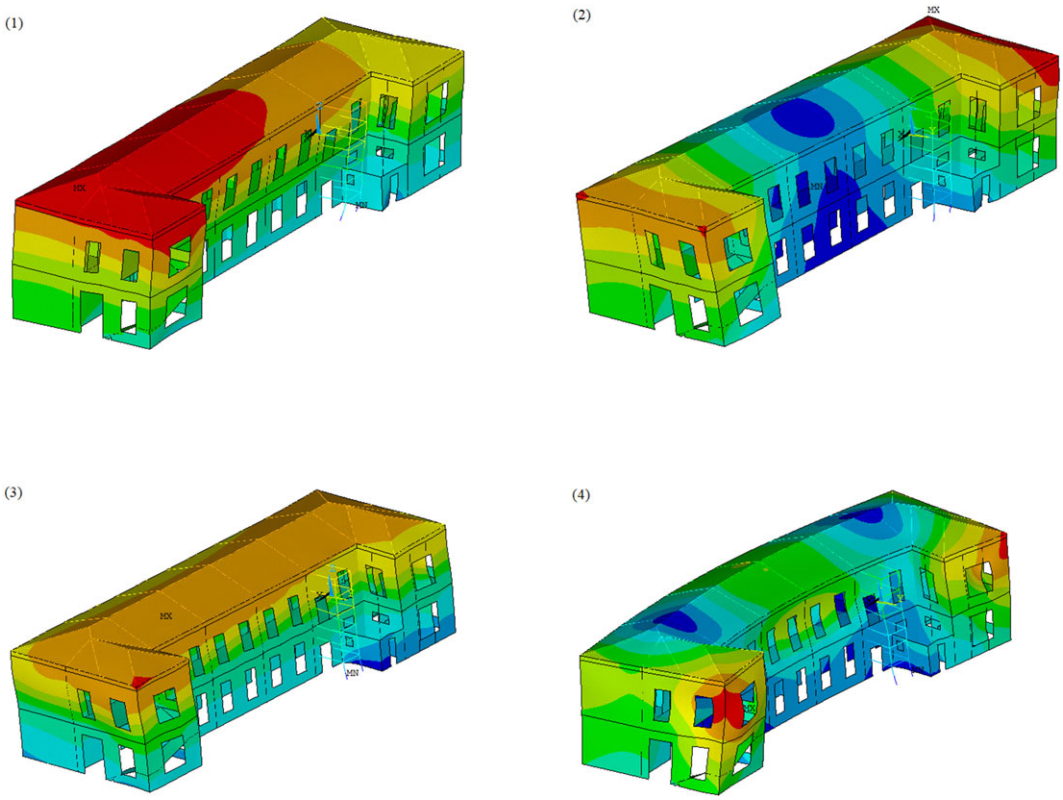

FIGURE 14 Updated numerical modal shapes; (1) first bending Y, (2) first torsional Z, (3) first bending X, (4) second torsional Z

TABLE 14 Numerical results found by the calibrations with PL selection

Quantity	Experimental values (exp.)				Numerical initial values (num.)				Numerical final values (num.)			
f_1 f_2 f_3 f_4 (Hz)	4.83	5.84	7.01	9.26	5.45	5.96	6.52	10.28	4.86	5.32	6.79	10.01
$\lvert f_{exp}\text{-}f_{num}/f_{exp}$	0	0	0	0	0.13	0.02	0.07	0.11	0.01	0.09	0.03	0.08
MAC	1.00	0.08	0.01	0.00	0.91	0.02	0.00	0.01	0.91	0.00	0.00	0.00
	0.08	1.00	0.02	0.02	0.14	0.78	0.08	0.02	0.03	0.89	0.02	0.02
	0.01	0.02	1.00	0.00	0.01	0.01	0.84	0.00	0.01	0.00	0.93	0.00
	0.00	0.02	0.00	1.00	0.05	0.01	0.00	0.90	0.05	0.02	0.00	0.93
E_7, E_9 (Pa)	Unknowns				2.800e9, 2.800e9				1.416e9, 4.435e9			
K_Y, K_X (N/m)					5.000e7, 5.000e7				2.559e7, 6.345e7			

Abbreviation: PL, Plackett-Luce.

was also validated by performing a sensitivity analysis, which confirmed that the frequencies are very sensitive to a variation of the chosen moduli and stiffness.

In this situation, the number of items, Q, of the calibration is four. The experimental measurements together with the starting values of the parameters and their searching space are reported in Tables 12 and 13. In Figure 14, instead, the first four updated numerical modal shapes are depicted, and the numerical values of the results in terms of frequencies (with the related errors), MAC, and optimal values of the parameters are reported in Table 14.

The results of the application to the Town Hall building of Pizzoli can be summarized as follows:

- The overall modal quantities (i.e., frequencies and modal shapes) tend to satisfactorily approach the experimental values, with an average error of 5.25% for the frequencies, and 8.50% for the MAC, ensuring a more realistic response of the model in the case of dynamic analysis;
- The stiffness of the springs turned out to be higher in the X direction than in the Y direction, in accordance with the greater stiffness of the foundation walls in the X direction;
- The Young's modulus of the walls at the raised floor level was attributed a higher value by PL than that of the higher levels. This may be due to (a) a different composition of the masonry for the walls of the higher floor in comparison with the walls of the raised ground floor and (b) the presence of damage in the first floor walls (due to the 2009 earthquake of L'Aquila). In order to differentiate the two cases, records prior to the earthquake of L'Aquila (2009) would be required. Another explanation, which should always be considered in inverse problems, can be found in the challenge of properly representing the deformability and inertia of the basement level, a challenge that is always present when dealing with structures like the Town Hall of Pizzoli.

5 | CONCLUSIONS

In the past several optimization algorithms, such as the MM algorithm, have been used to solve the RA problem to infer the parameters of specific distributions in a probabilistic framework. In this paper, we instead propose to use the RA strategy to solve optimization problems that are typically encountered in model updating and model-driven SHM. To do so, the use of combinatorial optimization methods has been investigated in order to establish a reference numerical model to support monitoring activities, as typically required by the seismic observatories of structures. In order to test the effectiveness of the combinatorial selection, based on a PL RA, the strategy was first applied to several well-known test functions, giving satisfactory results. The same procedure was then conducted on an FE benchmark problem. PL has proven to be an effective tool to increase the accuracy and the precision of the solution, while producing more reliable results.

In order to demonstrate the strategy on real dynamic monitoring data, the FE calibration of the Town Hall building of Pizzoli was carried out following four different optimization criteria: PSO, SA, PS, and GA. The results of the optimization were recursively treated, using a combinatorial strategy, by solving the RA problem with the PL model. Because of the high uncertainty, the calibration took into account the soil–structure interaction parameters, representing the part of the structure below the raised floor, and the Young's moduli of the masonry walls. The results show that, after the optimization and ranking procedure, the numerical modal quantities (i.e., frequencies

and modal shapes), satisfactory fit the experimental ones with an average error of 5.25% for the frequencies and 8.50% for the MAC.

To the best of the authors' knowledge, this is the first study that has employed RA strategies to achieve the optimal selection of a calibrated FEM. It is worth highlighting that the RA strategy can also be used in the selection of the best optimization parameters of a specific model updating algorithm, a concept broadly known as metaoptimization, or even to perform multiobjective optimizations.

ACKNOWLEDGEMENTS

The research was partially funded by an INTE project funded by Compagnia di San Paolo. Title of the project: "System Identification, model updating and damage assessment of heritage buildings and structures," partners: Politecnico di Torino and Columbia University (USA). The monitoring data of the Town Hall of Pizzoli were supplied by the "Seismic Observatory of Structures" (OSS) within the DPC-ReLUIS 2014-2018 PR.1 "Masonry Structures." The authors would like to thank Dr. Giulia De Lucia for her precious support connected to the ReLUIS activities.

ORCID

Gaetano Miraglia https://orcid.org/0000-0002-3611-0215
Erica Lenticchia https://orcid.org/0000-0002-3746-2933
Rosario Ceravolo https://orcid.org/0000-0001-5880-8457

REFERENCES

1. Bursi OS, Kumar A, Abbiati G, Ceravolo R. Identification, model updating, and validation of a steel twin deck curved cable-stayed footbridge. *Comput Aided Civ Inf Eng*. 2014;29(9):703-722.
2. Sun H, Betti R. A hybrid optimization algorithm with Bayesian inference for probabilistic model updating. *Comput Aided Civ Inf Eng*. 2015;30(8):602-619.
3. Boscato G, Russo S, Ceravolo R, Fragonara LZ. Global sensitivity-based model updating for heritage structures. *Comput Aided Civ Inf Eng*. 2015;30(8):620-635.
4. Ceravolo R, Pistone G, Fragonara LZ, Massetto S, Abbiati G. Vibration-based monitoring and diagnosis of cultural heritage: a methodological discussion in three examples. *Int J Architect Herit*. 2016;10(4):375-395.
5. Zhang F-L, Ni Y-C, Lam H-F. Bayesian structural model updating using ambient vibration data collected by multiple setups. *Struct Control Health Monit*. 2017;24(12):e2023.
6. Hu J, Lam H-F, Yang J-H. Operational modal identification and finite element model updating of a coupled building following Bayesian approach. *Struct Control Health Monit*. 2018;25(2):e2089.
7. Bassoli E, Vincenzi L, D'Altri AM, de Miranda S, Forghieri M, Castellazzi G. Ambient vibration-based finite element model updating of an earthquake-damaged masonry tower. *Struct Control Health Monit*. 2018;25(5):e2150.
8. Yasutake S, Hatano K, Takimoto E, Takeda M. Online rank aggregation, in Asian Conference on Machine Learning, pp. 539–553, 2012.
9. Cao Z, Qin T, Liu TY, Tsai MF, Li H. Learning to rank: from pairwise approach to listwise approach, in Proceedings of the 24th international conference on Machine learning, pp. 129–136, ACM, 2007.
10. Beggs S, Cardell S, Hausman J. Assessing the potential demand for electric cars. *J Econom*. 1981;17(1):1-19.
11. Gormley I, Murphy T. Exploring Irish election data: a mixture modelling approach, Technical Report 05/08, 2005.
12. Dwork C, Kumar R, Naor M, Sivakumar D. Rank aggregation methods for the web, in Proceedings of the 10th international conference on World Wide Web, pp. 613–622, ACM, 2001.
13. Fagin R, Kumar R, Sivakumar D. Efficient similarity search and classification via rank aggregation, in Proceedings of the 2003 ACM SIGMOD international conference on Management of data, pp. 301–312, ACM, 2003.
14. Andoni A, Fagin R, Kumar R, Patrascu M, Sivakumar D. Corrigendum to efficient similarity search and classification via rank aggregation by Ronald Fagin, Ravi Kumar and D. Sivakumar (proc. sigmod'03), in Proceedings of the 2008 ACM SIGMOD international conference on Management of data, pp. 1375–1376, ACM, 2008.
15. Marden JI. *Analyzing and Modeling Rank Data*. Chapman and Hall/CRC; 2014.
16. Guiver J, Snelson E. Bayesian inference for Plackett-Luce ranking models, in Proceedings of the 26th Annual International Conference on Machine Learning, pp. 377–384, ACM, 2009.
17. Plackett RL. The analysis of permutations. *Appl Stat*. 1975;24(2):193-202.
18. Luce RD. Individual choice behavior: a theoretical analysis. Courier Corporation, 2012.

19. Hunter DR et al. Mm algorithms for generalized Bradley-Terry models. *Ann Stat*. 2004;32(1):384-406.
20. Minka T. Power EP, tech. rep., Technical report, Microsoft Research, Cambridge, 2004.
21. Minka T et al. Divergence measures and message passing, tech. rep., Technical report, Microsoft Research, 2005.
22. Aledo JA, Gámez JA, Molina D. Tackling the rank aggregation problem with evolutionary algorithms. *Appl Math Comput*. 2013;222:632-644.
23. Aledo JA, Gámez JA, Molina D. Tackling the supervised label ranking problem by bagging weak learners. *Inf Fusion*. 2017;35:38-50.
24. MATLAB, The MathWorks, Inc., Natick, Massachusetts,United States, 2018.
25. Sun J, Feng B, Xu W. Particle swarm optimization with particles having quantum behavior. In Proceedings of the 2004 Congress on Evolutionary Computation (IEEE Cat. No. 04TH8753) (Vol. 1, pp. 325–331). 2004, June IEEE.
26. Yumin D, Li Z. Quantum behaved particle swarm optimization algorithm based on artificial fish swarm. *Math Probl Eng*. 2014;2014:1-10.
27. dos Santos Coelho L, Guerra FA, Pasquim B, Mariani VC. Chaotic quantum-behaved particle swarm optimization approach applied to inverse heat transfer problem. 2013 In IJCCI (pp. 97–102).
28. Joachims T, Li H, Liu T-Y, Zhai C. Learning to rank for information retrieval (lr4ir 2007). *Acm Sigir Forum*. 2007;41(2):58-62, ACM.
29. Patelli E, Govers Y, Broggi M, Gomes HM, Link M, Mottershead JE. Sensitivity or Bayesian model updating: a comparison of techniques using the DLR AIRMOD test data. *Arch Appl Mech*. 2017;87(5):905-925.
30. Yuan Z, Liang P, Silva T, Yu K, Mottershead JE. Parameter selection for model updating with global sensitivity analysis. *Mech Syst Signal Process*. 2019;115:483-496.
31. Goldberg DE. *Genetic Algorithms in Search, Optimization, and Machine Learning*. New York: Addison-Wesley; 1989.
32. Audet C, Dennis JE Jr. Analysis of generalized pattern searches. *SIAM J Optim*. 2002;13(3):889-903.
33. Kennedy J, Eberhart R. Particle swarm optimization, in Proceedings of ICNN'95—International Conference on Neural Networks, vol. 4, pp. 1942–1948 vol.4, Nov 1995.
34. Ingber L. Adaptive simulated annealing (ASA): lessons learned, arXiv preprint cs/0001018, 2000.
35. Bama SS, Ahmed MI, Saravanan A. A survey on performance evaluation measures for information retrieval system. *Int Res J Eng Technol*. 2015;2(2):1015-1020.
36. Sun W, Yuan Y-X. *Optimization Theory and Methods: Nonlinear Programming*. 1, LLC, 233 Spring Street, New York, NY 10013, USA: Springer Science & Business Media; 2006.
37. Mishra SK. Some new test functions for global optimization and performance of repulsive particle swarm method, 2006.
38. Dolce M, Nicoletti M, De Sortis A, Marchesini S, Spina D, Talanas F. Osservatorio sismico delle strutture: the Italian structural seismic monitoring network. *Bull Earthq Eng*. 2017;15(2):621-641.
39. Di Ludovico M, Digrisolo A, Graziotti F, et al. The contribution of ReLUIS to the usability assessment of school buildings following the 2016 central Italy earthquake. *Boll Geofis Teor Appl*. 2017;58(4).
40. Ceravolo R, Matta E, Quattrone A, Zanotti Fragonara L. Amplitude dependence of equivalent modal parameters in monitored buildings during earthquake swarms. *Earthq Eng Struct Dyn*. 2017;46(14):2399-2417.
41. Ceravolo R, De Lucia G, Matta E, Quattrone A, Zanotti Fragonara L. Equivalent modal parameters in monitored buildings during the recent Italian seismic events, in Atti del XVII Convegno ANIDIS L'ingegneria Sismica in Italia, pp. 21–30, Pisa University Press, 2017.
42. Van Overschee P, De Moor B. N4sid: subspace algorithms for the identification of combined deterministic-stochastic systems. *Automatica*. 1994;30(1):75-93.
43. Kim J, Lynch JP. Subspace system identification of support-excited structures—part i: theory and black-box system identification. *Earthq Eng Struct Dyn*. 2012;41(15):2235-2251.

How to cite this article: Miraglia G, Lenticchia E, Ceravolo R, Betti R. Synergistic and combinatorial optimization of finite element models for monitored buildings. *Struct Control Health Monit*. 2019;26:e2403. https://doi.org/10.1002/stc.2403